



Published in final edited form as:

*Genet Med.* 2021 August ; 23(8): 1474–1483. doi:10.1038/s41436-021-01158-1.

## Loss-of-function and missense variants in *NSD2* cause decreased methylation activity and are associated with a distinct developmental phenotype

Paolo Zaroni, M.D., Ph.D.<sup>#†,1</sup>, Katharina Steindl, M.D.<sup>#1</sup>, Deepanwita Sengupta, Ph.D.<sup>#2</sup>, Pascal Joset, Ph.D.<sup>1</sup>, Angela Bahr, Ph.D.<sup>1</sup>, Heinrich Sticht, Ph.D.<sup>3</sup>, Mariarosaria Lang-Muritano, M.D.<sup>4,5</sup>, Conny M.A. van Ravenswaaij-Arts, M.D., Ph.D.<sup>6</sup>, Marwan Shinawi, M.D.<sup>7</sup>, Marisa Andrews, M.S., C.G.C.<sup>7</sup>, Tania Attie-Bitach, M.D., Ph.D.<sup>8,9</sup>, Isabelle Maystadt, M.D., Ph.D.<sup>10,11</sup>, Newell Belnap, P.A.<sup>12,13</sup>, Valerie Benoit, Ph.D.<sup>10</sup>, Geoffroy Delplancq, M.Sc.<sup>14,15</sup>, Bert B.A. de Vries, M.D., Ph.D.<sup>16</sup>, Sarah Grotto, M.D.<sup>17</sup>, Didier Lacombe, M.D.<sup>18</sup>, Austin Larson, M.D.<sup>19</sup>, Jeroen Mourmans, M.D.<sup>20</sup>, Katrin Ōnap, M.D., Ph.D.<sup>21,22</sup>, Giulia Petrilli, M.D.<sup>8</sup>, Rolph Pfundt, Ph.D.<sup>16</sup>, Keri Ramsey, M.D.<sup>12,13</sup>, Lot Snijders Blok, M.D.<sup>16</sup>, Vassilis Tsatsaris, M.D., Ph.D.<sup>17</sup>, Antonio Vitobello, Ph.D.<sup>23</sup>, Laurence Faivre, M.D.<sup>24</sup>, Patricia G. Wheeler, M.D.<sup>25</sup>, Marijke R. Wevers, M.D., Ph.D.<sup>16</sup>, Monica Wojcik, M.D.<sup>26,27</sup>, Markus Zweier, Ph.D.<sup>1</sup>, Or Gozani, M.D., Ph.D.<sup>#2</sup>, Anita Rauch, M.D.<sup>#†,1,28,29</sup>

<sup>1</sup>Institute of Medical Genetics, University of Zürich, Schlieren-Zurich, 8952, Switzerland

<sup>2</sup>Department of Biology, Stanford University, Stanford, CA, 94305-5020, USA <sup>3</sup>Institute of

Biochemistry, Friedrich-Alexander University Erlangen-Nürnberg, Erlangen, 91054, Germany

<sup>4</sup>Department of Pediatric Endocrinology and Diabetology, University Children's Hospital, Zurich,

Users may view, print, copy, and download text and data-mine the content in such documents, for the purposes of academic research, subject always to the full Conditions of use:[http://www.nature.com/authors/editorial\\_policies/license.html#terms](http://www.nature.com/authors/editorial_policies/license.html#terms)

**Correspondence** All correspondence can be addressed to paolo.zaroni@uzh.ch (†) and anita.rauch@medgen.uzh.ch (††), +41 (0)44 556 33 00.

### Author contributions

Conceptualization: K.S., O.G., A.R.; Formal analysis: P.Z., D.S., H.S.; Funding acquisition: A.R., H.S., O.G., B.B.A.d.V.; Investigation: P.Z., K.S., D.S., H.S., P.J., A.B., M.L.M., C.M.A.R.-A., M.S., M.A., T.A.B., I.M., N.B., V.B., G.D., B.B.A.d.V., S.G., D.L., A.L., J.M., K.Ö., G.P., R.P., K.R., L.S.B., V.T., A.V., L.F., P.G.W., M.R.W., M.W., M.Z.; Project administration: P.Z., K.S., A.R., O.G.; Supervision: A.R., O.G.; Visualization: P.Z., D.S., H.S., P.G.; Writing – original draft: P.Z.; Writing – review & editing: K.S., D.S., A.R., H.S., O.G.

### Supplemental Data

Supplemental Data include Figure S1, Table S1, S2, S3 and S4, the clinical descriptions of each affected individual, and supplemental Materials and Methods.

### Data Availability

All materials, data sets, and protocols presented in this work are available upon request to the corresponding authors. *NSD2* variants have been deposited in the Decipher database (see Web Resources) under the following IDs: 422873, 422875, 422876, 422877, 422878, 422879, 422880, 422881, 422882, 422883, 422885, 422886, 422887, 422888, 422889, 422890, 422891, 422892.

### Ethics Declaration

This study was performed as part of a research study approved by the ethics commission of the Canton of Zurich (PB\_2016–02520). Written informed consent for genetic testing and publication of genetic and clinical data, and photos was obtained from each individual, their parents or their legal guardian. Genetic testing in collaborating centers was performed either in the setting of routine diagnostic without the requirement for IRB approval or within research settings, under the following approvals: p.3-I: Comité de Protection des Personnes (Dijon), # DC2011–1332; p.4-I: Colorado Multiple Institutional Review Board, #19–0751; p.5-I: Western Institutional Review Board, #20120789; p.15-I: #287/M-15, The Ethics Committee of University of Tartu.

### Conflict of Interest Statement

O.G. is a co-founder and member of the Board of Directors of EpiCypher, Inc.

8032, Switzerland <sup>5</sup>Children's Research Centre, University Children's Hospital, Zurich, 8032, Switzerland <sup>6</sup>University of Groningen, University Medical Centre Groningen, Department of Genetics, Groningen, 9713 GZ, The Netherlands <sup>7</sup>Department of Pediatrics, Division of Genetics and Genomic Medicine, Washington University School of Medicine, St. Louis, MO, 63110, USA <sup>8</sup>Service d'Histologie-Embryologie-Cytogénétique, Unité d'Embryofetopathologie, Hôpital Necker-Enfants Malades, APHP, Paris, 75015, France. <sup>9</sup>INSERM UMR 1163, Université de Paris, Imagine Institute, Paris, 75015, France <sup>10</sup>Centre de Génétique Humaine, Institut de Pathologie et de Génétique, Gosselies, 6041, Belgium <sup>11</sup>Faculté de médecine, Université de Namur, Namur, 5000, Belgium <sup>12</sup>Center for Rare Childhood Disorders (C4RCD), Translational Genomics Research Institute, Phoenix, AZ, 85004, USA <sup>13</sup>Neurogenomics Division, Translational Genomics Research Institute, Phoenix, AZ, 85004, USA <sup>14</sup>Centre de Génétique Humaine, Université de Franche-Comté, CHU, Besançon, 25030, France <sup>15</sup>Service de Neuropédiatrie, CHU, Besançon, 25000, France <sup>16</sup>Department of Human Genetics, Radboud University Medical Center, Nijmegen, 6525 GA, The Netherlands <sup>17</sup>Maternité Port-Royal, AP-HP, Hôpital Cochin, Paris, F-75014, France <sup>18</sup>Service de Génétique Médicale, Hôpital Pellegrin CHU, Bordeaux, 33076, France <sup>19</sup>Department of Pediatrics, Section of Genetics, University of Colorado Anschutz Medical Campus, Denver, CO, 80045, USA <sup>20</sup>Deventer Ziekenhuis, Deventer, 7416 SE, the Netherlands <sup>21</sup>Department of Clinical Genetics, United Laboratories, Tartu University Hospital, Tartu, 50406, Estonia <sup>22</sup>Department of Clinical Genetics, Institute of Clinical Medicine, University of Tartu, Tartu, 50406, Estonia <sup>23</sup>UFR Des Sciences de Santé, INSERM-Université de Bourgogne UMR1231 GAD, FHU-TRANSLAD, Unité Fonctionnelle D'Innovation en Diagnostique Génomique Des Maladies Rares, Pôle de Biologie, CHU Dijon Bourgogne, Dijon, 21000, France <sup>24</sup>Centre de Référence Maladies Rares « Anomalies du Développement Et Syndrome Malformatifs » de L'Est, Hôpital D'Enfants, FHU-TRANSLAD, CHU Dijon Bourgogne, Dijon, 21000, France <sup>25</sup>Division of Genetics, Arnold Palmer Hospital, Orlando Health, Orlando, FL, 32806, USA <sup>26</sup>Divisions of Newborn Medicine and Genetics and Genomics, Department of Pediatrics, Boston Children's Hospital, Boston, MA, 02115, USA <sup>27</sup>The Broad Institute of MIT and Harvard, Cambridge, MA, 02142, USA <sup>28</sup>Zurich Center for Integrative Human Physiology, University of Zurich, Zurich, 8000, Switzerland <sup>29</sup>Neuroscience Center Zurich, University of Zurich and ETH Zurich, Zurich, 8000, Switzerland

# These authors contributed equally to this work.

## Abstract

**Purpose:** Despite few recent reports of patients harbouring truncating variants in *NSD2*, a gene considered critical for the Wolf-Hirschhorn syndrome (WHS) phenotype, the clinical spectrum associated with *NSD2* pathogenic variants remains poorly understood.

**Methods:** We collected a comprehensive series of 18 unpublished patients carrying heterozygous missense, elongating or truncating *NSD2* variants, compared their clinical data to the typical WHS phenotype after pooling them with 10 previously described patients, and assessed the underlying molecular mechanism by structural modelling as well as by measuring methylation activity *in vitro*.

**Results:** The core *NSD2*-associated phenotype includes mostly mild developmental delay, prenatal-onset growth retardation, low BMI and characteristic facial features distinct from WHS. Patients carrying missense variants were significantly taller and had more frequent behavioural/psychological issues compared to those harbouring truncating variants. Structural *in silico* modelling suggested interference with *NSD2*'s folding and function for all missense variants in known structures. *In vitro* testing showed reduced methylation activity and failure to reconstitute H3K36me2 in *NSD2* knockout cells for most missense variants.

**Conclusions:** *NSD2* loss-of-function variants lead to a distinct, rather mild phenotype partially overlapping with WHS. To avoid confusion for patients, *NSD2* deficiency may be named after the delineators of this phenotype “Rauch-Steindl” syndrome.

## Introduction

Wolf-Hirschhorn Syndrome (WHS, also known as 4p- syndrome, OMIM 194190) caused by partial deletions of the short arm of chromosome 4 is one of the first microscopically recognized structural chromosomal disorders named after Ulrich Wolf from Freiburg, Germany, and Kurt Hirschhorn, New York, USA, who first described it in 1965<sup>1,2</sup>. Hallmarks of the syndrome are prenatal-onset growth deficiency, microcephaly, intellectual disability, epilepsy, muscular hypotonia and hypotrophy, facial clefts, congenital heart defects and other malformations, as well as a very characteristic craniofacial gestalt, often described as resembling a “Greek helmet”<sup>3</sup>. With the advent of molecular cytogenetics a number of patients with smaller deletions encompassing 4p16.3 were identified, with deletions below 3.5 Mb found to be associated with a milder phenotype without major malformations<sup>3</sup>. Following an observation by Dian Donnai<sup>4</sup>, Manchester, UK, individuals described as having Pitt-Rogers-Danks syndrome, were shown to also harbour 4p16.3 microdeletions sizing at least 3.7 Mb<sup>5</sup> and, as pointed out by Agatino Battaglia, Pisa, Italy, and John C. Carey, Salt Lake City, USA, are actually clinically indistinguishable from WHS.<sup>6</sup> Further refinement of the WHS critical region hinted at *NSD2* (also named *WHSC1* or *MMSET*, OMIM \*602952) as the gene possibly responsible for part of the manifestations of WHS, including growth retardation, intellectual disability and possibly susceptibility to infections<sup>7-10</sup>. This hypothesis was supported by a role for *NSD2* in neuronal development as well as in the regulation of cellular proliferation *in vitro*<sup>11-13</sup>. A total of 8 truncating, 2 splicing and 6 missense variants were listed among many others in sequencing studies of patient cohorts with neurodevelopmental disorders, growth abnormality or congenital heart defects without deep phenotyping information (Table S1).

Recently, eight individual patients with developmental delay and growth retardation carrying truncating or protein elongating variants in *NSD2* have been described<sup>14-18</sup>, with phenotypes that partially overlap with those of individuals carrying very small chromosomal deletions encompassing *NSD2*<sup>8-10</sup>.

However, the lack of larger systematic patient series and functional validation is hampering the understanding of the phenotype associated with *NSD2* constitutional variants. Here we report 18 additional deep-phenotyped individuals carrying heterozygous (likely) pathogenic *NSD2* variants, including a prenatal and two familial cases, together with *in silico* and *in*

*vitro* data providing insight into the underlying pathomechanism and genotype-phenotype correlations.

## Materials and Methods

The 18 previously undescribed patients with pathogenic *NSD2* variants reported in this study were identified by research or diagnostic exome or Mendeliome sequencing in various laboratories and collected via GeneMatcher (see Web Resources). When no developmental testing was performed, the degree of intellectual disability was estimated using the DSM-5 severity levels for intellectual disability (see Web Resources). Standard deviations scores for growth parameters were calculated based on the datasets provided by the Swiss Society of Pediatrics, which combine WHO, Swiss and German population data (see Web Resources). The facial overlay Figure 4B was obtained using the Face2Gene RESEARCH application (FDNA Inc., Boston, MA, USA) taking one frontal photo for each patient at the youngest available age.

*NSD2* variant nomenclature refers to the NM\_133330.2 transcript and pathogenicity classification is based on the ACMG guidelines<sup>19</sup>. Structural analysis of *NSD2* variants was performed using SwissModel, RasMol and Smart (see Web Resources). While the experimental crystal structure of the *NSD2* N-methyltransferase domain was available (Protein Data Bank, PDB: 5LSU), the PHD and PWWP domains were modelled using the homologous domains from TRIM24 (PDB: 4ZQL) and *NSD3* (PDB code: 2DAQ), respectively.

GST fusion proteins were obtained as described in the supplementary methods. *In vitro* methylation assays were performed as described in (Mazur et al., 2014)<sup>20</sup> and the supplemental methods using reagents listed in Table S2.

The data in Figure 2N, 2P, 2R and 2T are represented as mean  $\pm$ SD of two independent biological replicates. Statistical significance in 2N, 2P, 2R and 2T was tested by one-way analysis of variance (ANOVA) followed by two-tailed Dunnett's test without adjusting for multiple testing. The data in Figure 3C-E are represented as mean  $\pm$ SD. Groups in Figure 3E were compared by homoscedastic two-tailed Student's t-test after testing for equal variance by F-test.

---

### Web Resources

Decipher: <https://decipher.sanger.ac.uk>

DSM-5 severity levels for intellectual disability: <https://dsm.psychiatryonline.org/doi/full/10.1176/appi.books.9780890425596.dsm01>

Face2Gene: <https://www.face2gene.com/>

GeneMatcher: <https://genematcher.org>

gnomAD: <https://gnomad.broadinstitute.org/>

Growth curves of the Swiss society of pediatrics: <https://www.kispi.uzh.ch/de/zuweiser/broschueren/Seiten/document.axd?id=56c0bb56-1793-48f3-968e-238915f47bbd9>

HGMD Professional: <http://www.hgmd.cf.ac.uk/ac/index.php>

HPO: <https://hpo.jax.org/app/>

OMIM: <http://www.omim.org/>

PDB: <https://www.wwpdb.org>

RasMol: <http://www.openrasmol.org/>

Smart: <http://smart.embl-heidelberg.de/>

SwissModel: <https://swissmodel.expasy.org/>

Uniprot databank entry for *NSD2*: <https://www.uniprot.org/>; Entry O96028

The graphs in Figures 2N, 2P, 2R, 2T and 3A-F were generated using GraphPad Prism version 5.00 for Windows, (GraphPad Software, La Jolla California USA). All statistical analyses were performed with GraphPad Prism, except for F- and t-tests, which were performed using Microsoft© Excel.

## Results

We describe 18 patients, 16 of whom unrelated, carrying ultrarare (absent in gnomAD) pathogenic or likely pathogenic *NSD2* variants (Table S3). Of these, 6 carried 5 different missense variants while 12 carried 10 different truncating variants. 9 of the truncating and 4 of the missense variants were not reported before (Figure 1). Variant inheritance could not be determined in 4/18 cases, was confirmed parental in 3/18 cases and de novo in 11/18 cases.

*NSD2* is the principal enzyme that di-methylates histone H3 at lysine 36 (H3K36me2)<sup>11</sup> in most cell types and tissues<sup>21</sup>. H3K36me2 is an evolutionarily conserved histone modification linked to transcriptional activation. The (likely) pathogenic missense variants we found map to three distinct domains of *NSD2*. The Cys869Tyr (patient 1-I) substitution disrupts zinc binding within a PHD finger domain (residues 831–875) and hence induces improper folding and loss of function for this domain. Although the function of the *NSD2* PHD domain is unknown, these domains are virtually always found on chromatin-associated proteins and may function as epigenetic reader domains (Figure 2A and 2B). The Pro895Leu variant (patients 7-I and 7-II) is located in the core of one of *NSD2*'s PWWP domains (Figure 2C), another motif that generally functions as an epigenetic reader<sup>22</sup>. The leucine substitution at Pro895 is predicted to destabilize the domain through steric clashes with the adjacent Trp885 (Figure 2D).

All remaining missense variants are located within the methyltransferase domain of *NSD2*. Lys1019Arg (patient 12-I) is located in a loop of the methyltransferase domain that exhibits high local mobility or is entirely missing in the isolated *NSD2* crystal structure. This hampers reliable modelling but suggests that this region is flexible and might become stabilized upon protein-protein interactions, such as binding to the nucleosome substrate. Ser1137 is located in the domain's core (Figure 2E) and substitution to phenylalanine (p.Ser1137Phe, patient 10-I) is predicted to result in steric clashes with the adjacent Leu1163 residue (Figure 2F), leading to domain destabilization. Glu1091 forms a salt-bridge to Arg1160 in the wildtype structure (Figure 2G), which is disrupted due to the charge inversion in the Glu1091Lys variant (patient 5-I, Figure 2H). In addition, the longer Lys1091 sidechain forms steric clashes with Arg1160, which are expected to additionally destabilize the methyltransferase domain. To corroborate our *in silico* and *in vitro* data, we also tested previously functionally characterized substitutions within the methyltransferase domain, namely Glu1099Lys, Tyr1092Ala and Tyr1179Ala. Glu1099Lys is a recurrent variant found somatically in multiple cancer types including childhood leukemia and enhances methylation activity to alter global histone methylation<sup>23</sup>. Molecular modelling<sup>23</sup> suggested that the positively charged lysine may disrupt the favorable histone–enzyme interactions leading to a gain of function. Tyr1092Ala and Tyr1179Ala were not previously identified in patients but had been shown to abrogate catalytic activity based on homology to other

SET domain protein lysine methyltransferase enzymes<sup>11</sup>. Tyr1092 forms tight hydrophobic interactions with Leu1120 in the protein core (Figure 2I). Due to the shorter sidechain, these interactions are lost in the Ala1092 variant (Figure 2J) thereby predicted to destabilize the protein domain. Modeling of the Tyr1179Ala variant reveals that Tyr1179 forms direct interactions with the bound methyl donor S-adenosylmethionine (SAM, Figure 2K). These interactions are lost in the Tyr1179Ala mutant (Figure 2L), resulting in a predicted strong reduction of cofactor binding and hence loss of enzymatic activity. Based on these data, we postulated that one functional consequence of the *NSD2* missense variants identified in patients with developmental disorders might be disruption of NSD2's ability to generate H3K36me2.

To test this hypothesis, we determined H3K36me2 levels in HEK293T cells transiently transfected with *NSD2* wild-type or derivatives harbouring the various variants (Figures 2M and 2N). Consistent with previous work<sup>11,22</sup>, overexpression of wild-type *NSD2* and a cancer-related *NSD2* gain-of-function mutant (Glu1099Lys [E1099K])<sup>23</sup> caused a global increase in H3K36me2. Contrarily, the *NSD2* derivatives carrying variants observed in patients, apart from Cys869Tyr [C869Y] (patient 1-I) and Glu1091Lys [E1091K] (patient 5-I), significantly reduced the levels of H3K36me2 (Figure 2M; quantitation in Figure 2N). In particular, Ser1137Phe [S1137F] (patient 10-I) largely behaved like the negative control and the known *NSD2* catalytic mutant Tyr1179Ala [Y1179A] (Figures 2M and 2N). Given that Ser1137Phe (patient 10-I) is located within the SET domain, the data suggest that this variant causes direct impairment of NSD2's catalytic activity. To test this hypothesis, *in vitro* methylation assays were performed using a minimal domain of NSD2 that retains enzymatic activity<sup>11</sup> and recombinant nucleosomes as substrates. As shown in Figure 2O and 2Q (quantitation in 2P and 2R, respectively), Ser1137Phe (patient 10-I) abrogates NSD2's ability to methylate nucleosomes *in vitro* similarly to the previously characterized catalytic mutant Tyr1179Ala [Y1179A]), while Glu1091Lys (patient 5-I) and Lys1019Arg [K1019R] (patient 12-I) showed a modest reduction in methylation of nucleosomes (Figure 2O-2R). Cys869Tyr (patient 1-I) and Pro895Leu (patients 7-I and 7-II) lie outside of the minimal catalytic domain and thus could not be tested in this assay. Next, we used the CRISPR/Cas9 system to generate *NSD2*-depleted HT1080 cells, which leads to depletion of global H3K36me2, and then complemented these cells with CRISPR-resistant wild-type *NSD2* or the DD-associated *NSD2* variants to test their role in reconstituting physiologic levels of H3K36me2. In contrast to complementation with wild-type *NSD2* and gain-of-function *NSD2*-Glu1099Lys, cells complemented with the DD-associated *NSD2* variants were partially to largely compromised in their ability to rescue physiologic H3K36me2 levels, with Glu1091Lys (patient 5-I) being the only variant which did not reach statistical significance (Figures 2S and 2T). The Ser1137Phe variant (patient 10-I) completely failed to rescue, indicating that it essentially abolishes enzymatic activity. Overall, these data are consistent with all variants except Cys869Tyr (patient 1-I) compromising to varying degrees the ability of NSD2 to generate H3K36me2, a key epigenetic modification.

The main clinical features of the *NSD2*-cohort consisting of 18 individuals described here and 10 previously published individuals (8 carrying truncating or protein elongating variants<sup>14-18</sup> and two carrying a microdeletion that encompasses the *NSD2* gene, only<sup>10</sup>) are summarized in Figure 3A and compared to patients with WHS due to 4p deletions

of different sizes reported in a large series of 166 affected individuals<sup>3</sup> (Figure 3B). Post-mortem pathological findings for case 16-I, a male fetus whose pregnancy was terminated at the 27<sup>th</sup> week of gestation, are shown in Figure S1. Detailed clinical descriptions are provided in the supplement.

In the *NSD2*-cohort, the average age at last visit ( $\pm$ SD) was 9.3 ( $\pm$ 10.3) years and the male to female ratio was 18:10 (male 64%, female 36%). 75% of the *NSD2* variants were *de novo*, 14% were inherited from an affected parent, while in 11% of the cases, the inheritance pattern could not be established.

Patients with (likely) pathogenic *NSD2* variants shared a similar facial gestalt characterized by a triangular face, broad forehead, high anterior hairline, deeply set eyes, large palpebral fissures, broad arched and laterally sparse eyebrows, periorbital hyperpigmentation, full cheeks, a thin and elevated nasal bridge, smooth short philtrum, prominent cupid bow, thick everted lower lip vermilion and/or protruding ears (Figure 4A and 4B). Noticeably, the facial appearance evolved over time, with older patients developing deeper infraorbital creases. Family 6 comprised a total of 7 clinically similarly affected individuals, with molecular confirmation available for 4 of them, and represents to date the largest known family affected by this disorder (Figure 4C). The core phenotype of the *NSD2*-cohort (>50% of patients) is characterized by developmental delay, intrauterine growth retardation and low birth weight, feeding difficulties, failure to thrive, height and head circumference below the 5<sup>th</sup> centile ( $<$ -1.65 SDS), speech delay, and muscular hypotonia. Although these manifestations are present in WHS as well, the majority of the individuals in the *NSD2*-cohort lack many of the most common manifestations of WHS such as seizures<sup>3</sup>, orofacial clefts, coloboma as well as genital, cardiac and renal malformations and display a distinct facial phenotype that lacks the classical “Greek helmet” aspect. Furthermore, the severity of the intellectual disability in the *NSD2*-cohort was milder compared to patients carrying the most common 4p deletions (between 5 and 18Mb), which are severely affected in 76% of the cases<sup>3</sup>. While individuals 1-I, 13-I and 14-I harbouring the *NSD2* Cys869Tyr, p.Cys1183Valfs\*146 and p.Arg600\* variants respectively, either had an IQ in the lower-normal range (78–81 and 89, respectively) or presented with learning difficulties, individuals old enough for evaluation commonly showed mild ID, with only three individuals presenting with severe ID. The latter carried truncating variants (3-I c.3223\_3226dup p.Gly1076Valfs\*16; 4-I c.1588\_1589dupAA p.Ile532Glyfs\*67; Bernardini et al., patient 3, exon1–20 deletion), which may not be held responsible for the severe ID. Both siblings described as patient 2 and 3 in Bernardini et al. carry in fact the same exon 1–20 deletion, with one sibling showing mild ID, while the other had autism and severe ID<sup>10</sup>.

Behavioural and psychological issues as well as autistic features were observed in 44% and 33%, respectively, with the most frequently reported manifestations being anxiety (15%), hyperactivity (22%) and aggressiveness (11%). Individual 1-I had suicidal ideations related to his poor academic performance at the age of 11 years. Of note, all the individuals carrying missense variants presented with behavioural and psychological issues (Figure 3A), compared to 29% of patients with truncating variants or deletions (p-value = 0.0031 by two-tailed Fischer’s exact test).

Growth parameters at birth were largely below the norm (Figure 3C). Feeding difficulties were described in 52% of the affected individuals and may at least in part contribute to the failure to thrive. Short stature and growth retardation persisted later in life (Figure 3D). Delayed bone age was detected in 6 individuals (22%). Length and occipitofrontal circumference (OFC) at birth as well as all growth parameters at last visit were normally distributed according to a D'Agostino-Pearson omnibus normality test, while birth weight was skewed towards lower values ( $p = 0.0002$ ). Notably, heterozygotes for missense variants were significantly taller than patients carrying truncating variants as well as small deletions encompassing *NSD2* ( $p = 0.03$  by homoscedastic t-test after checking for comparable variance by F-test; Figure 3E) and none of them fell below the 5<sup>th</sup> centile for height at last visit. Weight and OFC at last visit were also higher in patients carrying missense variants, although this difference was not statistically significant ( $p=0.27$  and  $0.17$ , respectively). Finally, a linear regression analysis showed that older patients had significantly higher BMI values ( $r^2 = 0.1786$ ,  $p = 0.0396$ ; Figure 3F).

Gastrointestinal abnormalities were also quite common (43%), with constipation representing the most frequent manifestation (26%). Ophthalmological abnormalities were observed in 29% of patients and mostly included mild refraction defects and strabismus, while no individual presented with coloboma, which is considered a recurrent feature in WHS (see Figure 3B). One exception is represented by individual 3-I, who presented with bilateral keratoconus, retinitis pigmentosa and optic atrophy and received a corneal transplant at the age of 32. Reanalysis of her exome data revealed three rare variants of unknown significance in *RHO*, *KRT3* and *UNC45B* (Table S3), which were, however, maternally inherited and also present in her healthy sister. Skeletal and limb abnormalities were reported in 39% of the cases. Individual 12-I presented with a craniosynostosis that was surgically corrected at the age of 6 months, which may be explained by the patient's additional *de novo* heterozygous *AGO2* variant (Table S3). Also, of note, individual 7-II presented with 11 ossified ribs and 6 non rib-bearing lumbar vertebrae. Dental abnormalities were also quite frequent (32%). Brain and spinal cord malformations were present in 5 individuals (18%) and were mostly of minor importance except for individual 16-I, that presented with vermis hypoplasia. Less frequent manifestations among patients carrying *NSD2* pathogenic variants included a history of aspiration, cardiac and renal anomalies, neonatal jaundice, sleep disturbances, hearing loss, genital abnormalities and orofacial clefts (Table S3). Immunological abnormalities as well as recurrent infections, which represent a common morbidity and mortality cause in WHS<sup>24</sup>, were infrequent in the *NSD2*-cohort, where patient 5-I presented with latex allergy, patient 11-I with low IgA and IgG<sub>3</sub> levels and patients 2-I, 11-I and Derar-1 with recurrent respiratory infections. Seizures, which are common in WHS (Figure 3B), were reported only in individual 10-I, while individual 15-I presented subclinical EEG-abnormalities at the age of 4 4/12 years. Endocrinological abnormalities seem not to be part of the phenotypic spectrum, with only individual 5-I presenting limited signs of precocious puberty at 15 months of age, which were non-progressive and were associated with a normal endocrine evaluation. Likewise, metabolic abnormalities were only observed in individual 2-I.



## Discussion

In this work we describe a large series of patients carrying pathogenic variants in *NSD2*, thus allowing delineation of the associated manifestations, which include prenatal-onset failure to thrive with all body measurements below the mean and low BMI, mild developmental delay and muscular hypotonia, and a distinct facial gestalt. Furthermore, we provide *in silico* and *in vitro* mechanistic data showing loss of histone methylation activity as a common feature of *NSD2* deficiency.

The phenotype observed in the *NSD2*-cohort is consistent with many of the known functions of *NSD2*. First, *NSD2* has long been known to regulate embryonic development and body growth, with heterozygous *Nsd2* constitutive knockout mice growing at a much slower rate compared to wild type littermates, homozygous knockout mice dying in the first days of life<sup>25</sup>, and common variants showing strong ( $p=10^{-24}$ ) association with height in GWAS studies<sup>26</sup>. Recently *NSD2* was shown to regulate adipose tissue development in mice by controlling the activity of the master adipogenic transcription factor peroxisome proliferator-activated receptor- $\gamma$  (PPAR $\gamma$ )<sup>27</sup>. Interestingly, in this work mice overexpressing the mutant histone protein H3.3K36M, an *NSD2* inhibitor, resisted white adipose tissue expansion in response to a high-fat diet. These findings support the idea that the low BMI observed in the *NSD2*-cohort may be due to the inability of body fat to expand in response to feeding rather than a consequence of the neonatal feeding difficulties that, although observed in multiple affected individuals, disappear later in life. Furthermore, *NSD2* has been shown to play a key role in promoting adipogenesis and myogenesis in precursor cells, as well as thermogenesis in brown adipose tissue and insulin sensitivity in white adipose tissue<sup>27</sup>. In pancreatic beta-cell lines *in vitro* *NSD2* has also been shown to promote proliferation and to regulate insulin secretion<sup>28</sup>. However, since diabetes has not been reported as a recurrent feature neither in our cohort nor in patients with WHS we assume that in humans, glycaemic control may be maintained despite impaired *NSD2* function.

Likewise, some other known or supposed functions of *NSD2* did not result in a recurrent phenotype in our cohort. *NSD2* has been suggested to contribute to the immune defects typical of WHS by regulating the hematopoietic process at multiple stages as well as B-<sup>29</sup> and T-cell<sup>30</sup> differentiation. Nevertheless, only a minority of the patients in this series presented with recurrent infections. Also, while heterozygous *Nsd2* deficient mice present with heart defects<sup>25</sup> and *de novo* variants in *NSD2* were shown to associate with congenital heart malformations<sup>31</sup>, cardiac anomalies were present only in a minority of the individuals in this series and, with the exception of individual 16-I, were of minor clinical importance. The low prevalence of epilepsy in this cohort is compatible with the assumption that other genes such as *LETM1* are responsible for seizures in WHS<sup>32,33</sup>.

While heterozygotes for missense variants were on average significantly taller, the overall clinical severity correlated only loosely with the measured alteration in *NSD2* enzymatic function. Furthermore, for the Cys869Tyr (patient 1-I) variant, which can be categorized as likely pathogenic based on the current ACMG recommendations, we did not detect significant loss of methylation activity in our *in vitro* assays. These data suggest that in addition to H3K36 dimethylation, other functions of *NSD2* such as e.g. its genomic

localization, and likely other potential genetic differences amongst the patients, contribute to the pathogenesis of the complex phenotypes described here. Moreover, as the missense variants that we tested did not display any obvious stability issue upon overexpression, dominant negative effects cannot be excluded. Finally, second hits or blending phenotypes with additional variants in other (known or unknown) genes associated with the clinical phenotypes described in this study could contribute to the observed clinical variability.

Patients 11-I and 15-I carried the same protein-elongating p.Pro1343Glnfs\*49 variant. Although this variant occurs too distally in the mRNA sequence to induce nonsense-mediated decay, its pathogenicity is supported by the fact that this variant, together with the previously described p.Glu1344Lysfs\*49 variant<sup>18</sup>, all occurred *de novo* in similarly affected individuals. Although some of the patients in this series carried additional rare variants, none of these are likely pathogenic. Individual 1-I carries a 441Kb heterozygous interstitial microduplication in 22q11.2 (hg19 (chr22:22,817,344 – 23,258,369) which does not contain any disease-associated genes and was inherited from his healthy father. Individual 5-I carried the recurrent 312 kb interstitial duplication at 15q11.2 (hg19: 22,770,421 – 23,082,328) which was inherited from her healthy mother. In a large study on the effect of CNVs on cognition, 136 control individuals carrying the 15q11.2 duplication performed to a similar level as population controls on all tests of cognitive function<sup>34</sup>. In Family 7, where both mildly affected siblings (individual 7-I and 7-II) inherited the *NSD2* variant from their similarly affected mother, we additionally found that Individual 7-I carries a paternally inherited 783 kb deletion at 9p13.3 (hg19: 35,487,232–36,270,255) as well as the maternally-inherited *GABBR2* c.1656\_1657delTT, p.Cys553Hisfs\*96 variant. Her father had learning disability and depression. No overlapping deletion was present in the Decipher database but, based on the gene content and on the family history, a modulatory role of the 9p13.3 deletion on her phenotype cannot be excluded. Except for one truncating variant described in a large sequencing study on patients with neurodevelopmental delay<sup>35</sup>, all *GABBR2* pathogenic variants described until now in this gene are missense (source: HGMD Professional, release 2020.2, see Web Resources). This, together with the fact that her similarly affected brother (individual 7-II) didn't carry the p.Cys553Hisfs\*96 *GABBR2* variant speaks against a determining role on the phenotype. Individual 10-I carries a 38kb partial *HUWE1* duplication in Xp11.2, which overlaps with a recurrent polymorphic copy-number variant that does not affect the expression of *HUWE1* and thus should have no effect on cognition<sup>36</sup>.

Our study leaves unanswered questions for future research, such as the clarification of the full molecular mechanisms. This may reveal potential targets for therapeutic interventions not only relevant to patients with *NSD2* deficiency, but potentially even to patients with obesity in general.

In conclusion, our data support the concept that *NSD2* loss of function is associated with a distinct phenotype that only partially overlaps with WHS and constitutes a differential diagnosis to Silver-Russell and similar syndromes. This phenotype is in line with the distinct features described in the first patient with a small deletion encompassing *NSD2* by Rauch et al.<sup>8</sup>. This patient now at age 26 years is 172 cm tall (-0.55 SDS), weighs 45–50 Kg (ca. -2.5 SDS) and has a “small head”. Despite his normal eating behaviour, all attempts

to gain weight were unsuccessful. He has an IQ in the lower normal range, a calm and content personality and lives with his parents. As a reflection of the distinct facial gestalt and the greatly different disease severity, especially concerning intellectual disability, of *NSD2*-deficiency and contiguous gene deletions leading to WHS, which may also be important for families' and physician's perception of the patients' prognosis, the *NSD2*-related disorder may be named after the delineators of this phenotype "Rauch-Steindl" syndrome<sup>8</sup>.

## Supplementary Material

Refer to Web version on PubMed Central for supplementary material.

## Acknowledgements

The project was supported in part by the Swiss National Science Foundation grant 320030\_179547 to A.R., by RO1 grant GM079641 from the NIH to O.G., by grants from the Dutch Organization for Health Research and Development (ZON-MW grants 917–86–319 and 912–12–109 to B.B.A.d.V.) and by grants from the Estonian Research Council (grants PUT355 and PRG471 to K.Õ.). D.S. was supported by a grant from Stanford Maternal and Child Health Research Institute. A.R. and H.S. were supported by the UZH Clinical Research Priority Program Praeclare. The Broad Center for Mendelian Genomics (UM1 HG008900) is funded by the National Human Genome Research Institute with supplemental funding provided by the National Heart, Lung, and Blood Institute under the Trans-Omics for Precision Medicine (TOPMed) program and the National Eye Institute. C.M.A.R.-A., B.B.A.d.V., D.L., R.P., L.S.B. and M.R.W. are members of the European Reference Network on Rare Congenital Malformations and Rare Intellectual Disability ERN-ITHACA [EU Framework Partnership Agreement ID: 3HP-HP-FPA ERN-01–2016/739516].

## References

1. Wolf U, Reinwein H, Porsch R, Schröter R, Baitsch H. [Deficiency on the short arms of a chromosome No. 4]. *Humangenetik*1965;1(5):397–413. [PubMed: 5868696]
2. Hirschhorn K, Cooper HL, Firschein IL. Deletion of short arms of chromosome 4–5 in a child with defects of midline fusion. *Humangenetik*1965;1(5):479–482. doi:10.1007/BF00279124 [PubMed: 5895684]
3. Zollino M, Murdolo M, Marangi G, et al. On the nosology and pathogenesis of Wolf-Hirschhorn syndrome: Genotype-phenotype correlation analysis of 80 patients and literature review. *Am J Med Genet Part C Semin Med Genet*2008;148(4):257–269. doi:10.1002/ajmg.c.30190
4. Donnai D. Editorial comment: Pitt-Rogers-Danks syndrome and Wolf-Hirschhorn syndrome. *Am J Med Genet*1996;66(1):101–103. doi:10.1002/(SICI)1096-8628(19961202)66:1<101::AID-AJMG27>3.0.CO;2-V [PubMed: 8957525]
5. Kant SG, Van Haeringen A, Bakker E, et al. Pitt-Rogers-Danks syndrome and Wolf-Hirschhorn syndrome are caused by a deletion in the same region on chromosome 4p16.3. *J Med Genet*1997;34(7):569–572. doi:10.1136/jmg.34.7.569 [PubMed: 9222965]
6. Battaglia A, Carey JC. Wolf-Hirschhorn syndrome and Pitt-Rogers-Danks syndrome. *Am J Med Genet*1998;75(5):541. doi:10.1002/(sici)1096-8628(19980217)75:5<541::aid-ajmg18>3.0.co;2-k [PubMed: 9489803]
7. Wright TJ, Ricke DO, Denison K, et al. A transcript map of the newly defined 165 kb Wolf-Hirschhorn syndrome critical region. *Hum Mol Genet*1997;6(2):317–324. doi:10.1093/hmg/6.2.317 [PubMed: 9063753]
8. Rauch A, Schellmoser S, Kraus C, et al. First known microdeletion within the Wolf-Hirschhorn syndrome critical region refines genotype-phenotype correlation. *Am J Med Genet*2001;99(4):338–342. doi:10.1002/ajmg.1203 [pii] [PubMed: 11252005]
9. Okamoto N, Ohmachi K, Shimada S, Shimojima K, Yamamoto T. 109kb deletion of chromosome 4p16.3 in a patient with mild phenotype of Wolf-Hirschhorn syndrome. *Am J Med Genet Part A*2013;161(6):1465–1469. doi:10.1002/ajmg.a.35910

10. Bernardini L, Radio FC, Acquaviva F, et al. Small 4p16.3 deletions: Three additional patients and review of the literature. *Am J Med Genet Part A* 2018;176(11):2501–2508. doi:10.1002/ajmg.a.40512 [PubMed: 30244530]
11. Kuo AJ, Cheung P, Chen K, et al. NSD2 links dimethylation of histone H3 at lysine 36 to oncogenic programming. *Mol Cell* 2011;44(4):609–620. doi:10.1016/j.molcel.2011.08.042 [PubMed: 22099308]
12. Gabriele M, Lopez Tobon A, D'Agostino G, Testa G. The chromatin basis of neurodevelopmental disorders: Rethinking dysfunction along the molecular and temporal axes. *Prog Neuro-Psychopharmacology Biol Psychiatry* 2018;84:306–327. doi:10.1016/j.pnpbp.2017.12.013
13. Yang P, Guo L, Duan ZJ, et al. Histone methyltransferase NSD2/MMSET mediates constitutive NF- $\kappa$ B signaling for cancer cell proliferation, survival, and tumor growth via a feed-forward loop. *Mol Cell Biol* 2012;32(15):3121–3131. doi:10.1128/MCB.00204-12 [PubMed: 22645312]
14. Lozier ER, Konovalov FA, Kanivets I V., et al. De novo nonsense mutation in WHSC1 (NSD2) in patient with intellectual disability and dysmorphic features. *J Hum Genet* 2018;63(8):919–922. doi:10.1038/s10038-018-0464-5 [PubMed: 29760529]
15. Boczek NJ, Lahner CA, mi Nguyen T, et al. Developmental delay and failure to thrive associated with a loss-of-function variant in WHSC1 (NSD2). *Am J Med Genet Part A* 2018;176(12):2798–2802. doi:10.1002/ajmg.a.40498 [PubMed: 30345613]
16. Derar N, Al-Hassnan ZN, Al-Owain M, et al. De novo truncating variants in WHSC1 recapitulate the Wolf–Hirschhorn (4p16.3 microdeletion) syndrome phenotype. *Genet Med* 2019;21(1):185–188. doi:10.1038/s41436-018-0014-8 [PubMed: 29892088]
17. Barrie ES, Alfaro MP, Pfau RB, et al. De novo loss-of-function variants in NSD2 ( WHSC1 ) associate with a subset of Wolf–Hirschhorn syndrome. *Mol Case Stud* 2019;5(4):a004044. doi:10.1101/mcs.a004044
18. Jiang Y, Sun H, Lin Q, et al. De novo truncating variant in NSD2 gene leading to atypical Wolf-Hirschhorn syndrome phenotype. *BMC Med Genet* 2019;20(1):134. doi:10.1186/s12881-019-0863-2 [PubMed: 31382906]
19. Richards S, Aziz N, Bale S, et al. Standards and guidelines for the interpretation of sequence variants: A joint consensus recommendation of the American College of Medical Genetics and Genomics and the Association for Molecular Pathology. *Genet Med* 2015;17(5):405–424. doi:10.1038/gim.2015.30 [PubMed: 25741868]
20. Mazur PK, Reynoird N, Khatri P, et al. SMYD3 links lysine methylation of MAP3K2 to Ras-driven cancer. *Nature* 2014;510(7504):283–287. doi:10.1038/nature13320 [PubMed: 24847881]
21. Husmann D, Gozani O. Histone lysine methyltransferases in biology and disease. *Nat Struct Mol Biol* 2019;26(10):880–889. doi:10.1038/s41594-019-0298-7 [PubMed: 31582846]
22. Sankaran SM, Wilkinson AW, Elias JE, Gozani O. A PWWP Domain of histone-lysine N-methyltransferase NSD2 binds to dimethylated lys-36 of histone H3 and regulates NSD2 function at chromatin. *J Biol Chem* 2016;291(16):8465–8474. doi:10.1074/jbc.M116.720748 [PubMed: 26912663]
23. Oyer JA, Huang X, Zheng Y, et al. Point mutation E1099K in MMSET/NSD2 enhances its methyltransferase activity and leads to altered global chromatin methylation in lymphoid malignancies. *Leukemia* 2014;28(1):198–201. doi:10.1038/leu.2013.204 [PubMed: 23823660]
24. Shannon NL, Maltby EL, Rigby AS, Quarrell OWJ. An epidemiological study of Wolf-Hirschhorn syndrome: Life expectancy and cause of mortality. *J Med Genet* 2001;38(10):674–679. doi:10.1136/jmg.38.10.674 [PubMed: 11584045]
25. Nimura K, Ura K, Shiratori H, et al. A histone H3 lysine 36 trimethyltransferase links Nkx2–5 to Wolf-Hirschhorn syndrome. *Nature* 2009;460(7252):287–291. doi:10.1038/nature08086 [PubMed: 19483677]
26. Kichaev G, Bhatia G, Loh PR, et al. Leveraging polygenic functional enrichment to improve GWAS power. *Am J Hum Genet* 2019;104(1):65–75. doi:10.1016/j.ajhg.2018.11.008 [PubMed: 30595370]
27. Zhuang L, Jang Y, Park Y-K, et al. Depletion of Nsd2-mediated histone H3K36 methylation impairs adipose tissue development and function. *Nat Commun* 2018;9(1):1796. doi:10.1038/s41467-018-04127-6 [PubMed: 29728617]

28. Shi S, Zhao L, Zheng L. NSD2 is downregulated in T2DM and promotes  $\beta$  cell proliferation and insulin secretion through the transcriptionally regulation of PDX1. *Mol Med Rep* 2018;18(3):3513–3520. doi:10.3892/mmr.2018.9338 [PubMed: 30066931]
29. Campos-Sanchez E, Deleyto-Seldas N, Dominguez V, et al. Wolf-Hirschhorn syndrome candidate 1 is necessary for correct hematopoietic and B cell development. *Cell Rep* 2017;19(8):1586–1601. doi:10.1016/j.celrep.2017.04.069 [PubMed: 28538178]
30. Long X, Zhang L, Zhang Y, et al. Histone methyltransferase Nsd2 is required for follicular helper T cell differentiation. *J Exp Med* 2019. doi:10.1084/jem.20190832
31. Jin SC, Homsy J, Zaidi S, et al. Contribution of rare inherited and de novo variants in 2,871 congenital heart disease probands. *Nat Genet* 2017;49(11):1593–1601. doi:10.1038/ng.3970 [PubMed: 28991257]
32. Hart L, Rauch A, Carr AM, Vermeesch JR, O’Driscoll M. LETM1 haploinsufficiency causes mitochondrial defects in cells from humans with Wolf-Hirschhorn syndrome: Implications for dissecting the underlying pathomechanisms in this condition. *DMM Dis Model Mech* 2014;7(5):535–545. doi:10.1242/dmm.014464 [PubMed: 24626991]
33. Ho KS, South ST, Lortz A, et al. Chromosomal microarray testing identifies a 4p terminal region associated with seizures in Wolf-Hirschhorn syndrome. *J Med Genet* 2016;53(4):256–263. doi:10.1136/jmedgenet-2015-103626 [PubMed: 26747863]
34. Stefansson H, Meyer-Lindenberg A, Steinberg S, et al. CNVs conferring risk of autism or schizophrenia affect cognition in controls. *Nature* 2014;505(7483):361–366. doi:10.1038/nature12818 [PubMed: 24352232]
35. Kosmicki JA, Samocha KE, Howrigan DP, et al. Refining the role of de novo protein-truncating variants in neurodevelopmental disorders by using population reference samples. *Nat Genet* 2017;49(4):504–510. doi:10.1038/ng.3789 [PubMed: 28191890]
36. Froyen G, Belet S, Martinez F, et al. Copy-number gains of HUWE1 due to replication- and recombination-based rearrangements. *Am J Hum Genet* 2012;91(2):252–264. doi:10.1016/j.ajhg.2012.06.010 [PubMed: 22840365]

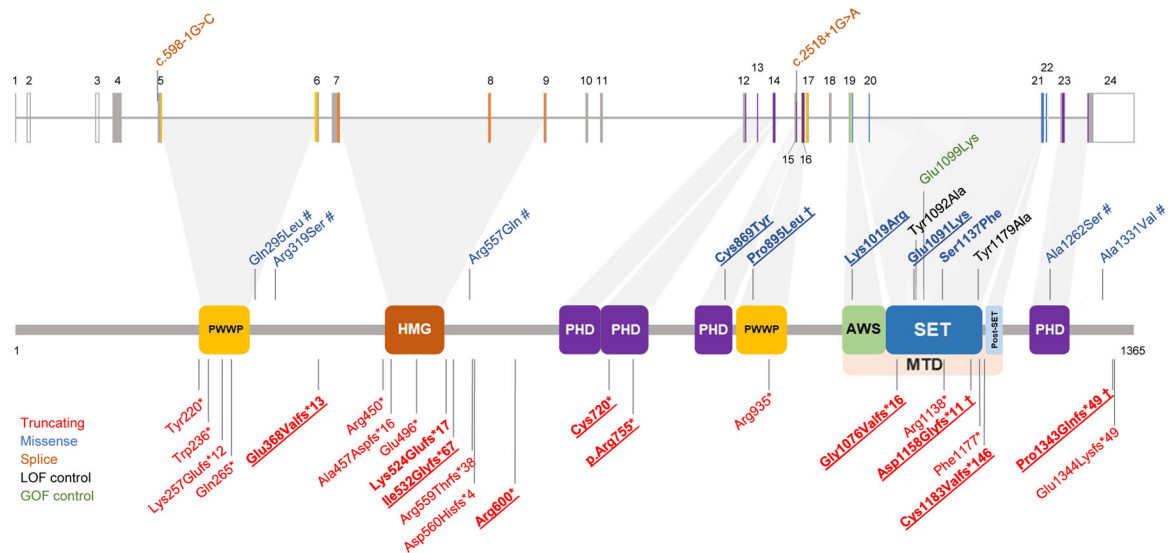


**Figure 1. Localization of the *NSD2* variants.**

The diagram shows the structure of the *NSD2* gene (above) and protein (below, isoform 1, encoded by the NM\_133330.2 transcript) together with the variants discussed in this study as well as variants that have previously been reported in large sequencing studies. The variants carried by the 18 additional individuals described in this study are in bold. Observed germline variants absent in the HGMD database are underlined. † = shared by more than one patient; # = VUS/likely benign. The observed pathogenic missense variants we found map to three distinct domains of *NSD2*: a PHD zinc-finger domain (residues 831–875), a PWWP domain (residues 880–942) and the catalytic methyltransferase domain (residues 1011–1203; composed of three subdomains, namely an AWS, a SET and a post-SET domain). The colour coding of the variants and protein domains is reported in the legend. PWWP: proline–tryptophan–tryptophan–proline domain (IPR000313); HMG: high mobility group box domain (IPR009071); PHD: zinc-finger domain, Plant-HomeoDomain type (IPR001965); AWS: Associated With SET domain (IPR006560); SET: Su(Var)3–9, enhancer-of-zeste, trithorax domain (IPR001214); MTD: catalytic methyltransferase domain, composed by the AWS, SET and a post-SET domain. Domains were annotated according to the Uniprot databank (see Web Resources).

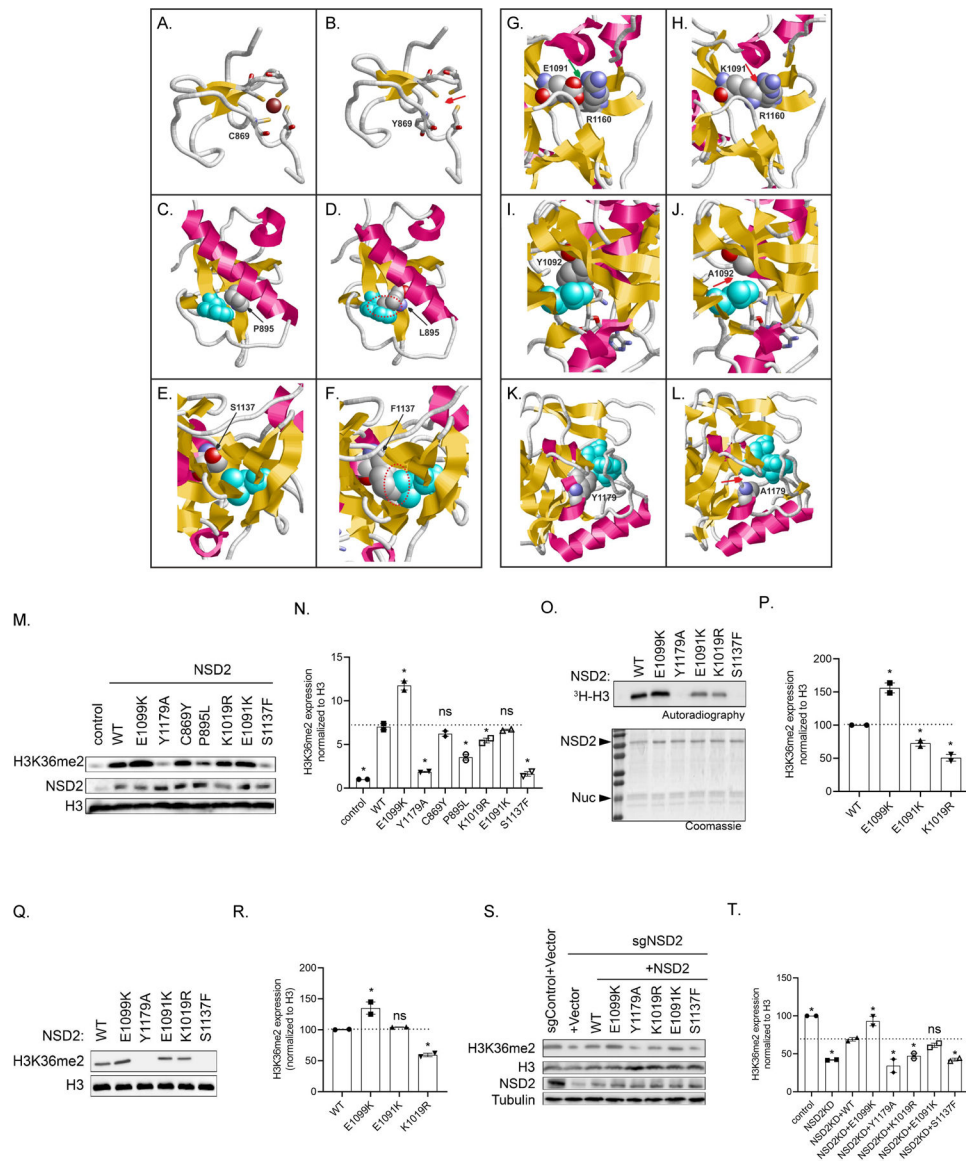


**Figure 2: Structural and functional effect of 2 synthetic and 4 naturally occurring pathogenic NSD2 missense variants.**

**A.** Wildtype Cys869 is one of four cysteines that tetrahedrally coordinate a zinc ion (Cys846, Cys849, Cys869, Cys872 are shown in stick presentation; the Zn<sup>2+</sup> is depicted as a brown ball). **B.** The variant Tyr869 adopts a different sidechain orientation resulting in a loss of the zinc ion (marked by a red arrow). **C.** Wildtype Pro895 is located in spatial proximity of Trp885 (cyan). **D.** The longer Leu895 sidechain present in the variant results in steric clashes with Trp885 (marked by a red dotted circle). **E.** Wildtype Ser1137 is located in spatial proximity of Leu1163 (cyan). **F.** The bulkier Phe1173 sidechain present in the variant results in steric clashes with Leu1163 (marked by a red dotted circle). **G.** Wildtype Glu1091 forms a salt-bridge to Arg1160 (green arrow), which is disrupted in the **(H)** Lys1091 variant and steric clashes are formed instead (red arrow). **I.** Wildtype Tyr1092 forms tight van-der-Waals interactions with Leu1120 (cyan), which are lost in the synthetic **(J)** Ala1092 variant<sup>11</sup> (the site of altered interactions is denoted by a red arrow).

**K.** Wildtype Tyr1179 forms stabilizing interactions to S-adenosylmethionine (SAM, cyan). **L.** The shorter sidechain in the synthetic Ala1179 variant<sup>11</sup> results in a loss of interactions with the SAM cofactor (red arrow), which is expected to result in a drastic loss of enzymatic activity. **M.** Western analysis with the indicated antibodies of whole cell extracts (WCEs) from 293T cells over-expressing vector control, full-length wild-type NSD2, or NSD2 mutants as indicated. Histone H3 is shown as a loading control. **N.** Quantification of Western blot data in **(M)**. **O.** *In vitro* methylation assay with recombinant wild-type NSD2 or mutant NSD2 derivatives as indicated on recombinant nucleosomes (rNuc) as substrates. Top panel, <sup>3</sup>H-SAM is the methyl donor and methylation is visualized by autoradiography and indicated as <sup>3</sup>H-H3. Bottom panel, Coomassie stain of proteins in the reaction. **P.** Quantification of all detectable bands in the autoradiography in **(O)**. **Q.** Western analysis with the indicated antibodies of *in vitro* methylation assay with non-radiolabeled SAM. **R.** Quantification of all detectable bands in the Western blot data in **(Q)**. **S.** Western analysis with the indicated antibodies of WCEs from wild-type or *NSD2* deficient HT1080 cells complemented with CRISPR-resistant *NSD2* (WT or mutants), or control as indicated. Histone H3 and tubulin are shown as loading controls. **T.** Quantification of Western blots in **(S)**. The data in **N, P, R and T** are represented as mean  $\pm$ SD of two independent experiments. \*= $p < 0.05$  based on a one-way ANOVA followed by two-tailed Dunnett's test.



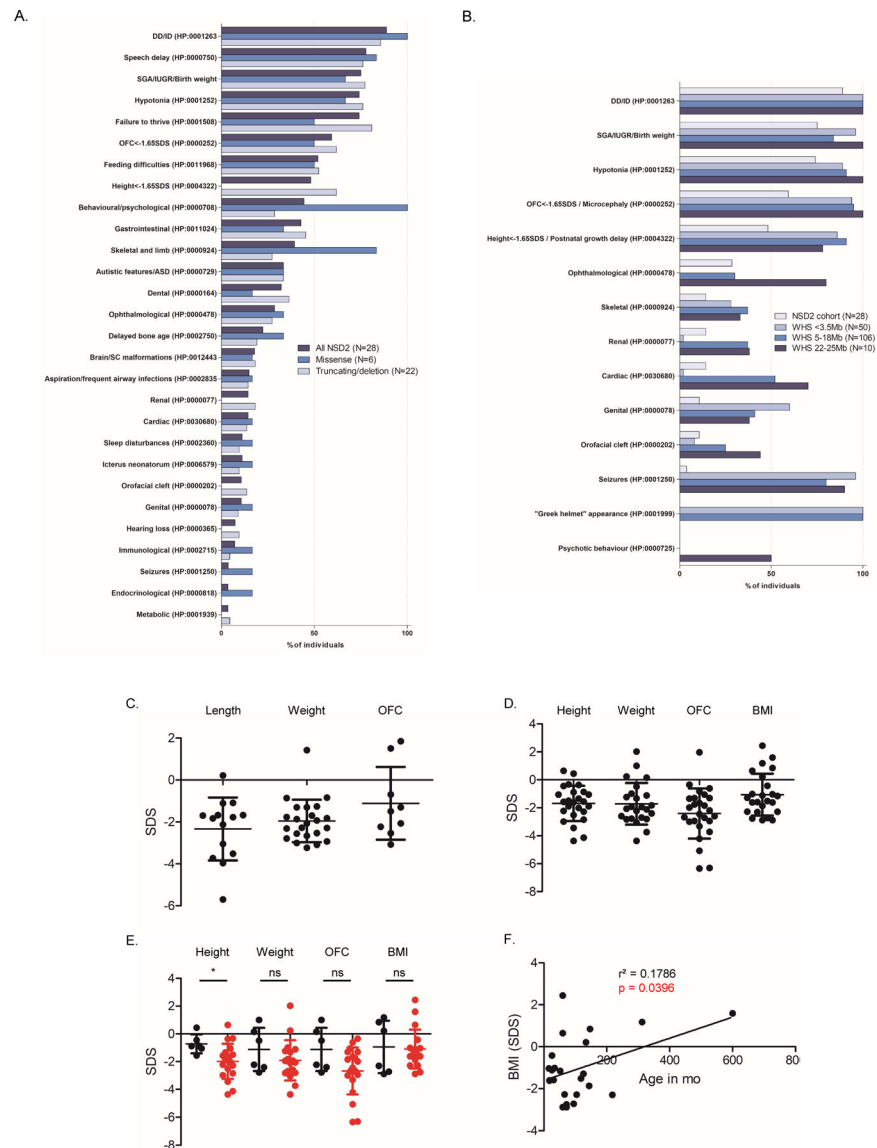


**Figure 3. Phenotypic features and growth parameters of the individuals carrying *NSD2* pathogenic variants and comparison with WHS.**

The diagram in **A** summarizes the phenotypic features of the individuals described in this study (18 additional patients together with 10 previously reported individuals) based on the type of *NSD2* variant carried. In **B** all individuals are compared with Wolf-Hirschhorn syndrome patients, subdivided according to the size of the 4p deletion carried, as reported in Zollino et al., American Journal of Medical Genetics, 148C:257–269, 2008. Data in **A** and **B** are expressed as percentages. Growth parameters at birth (**C**; included the parameters at termination of pregnancy for individual 16-I) and at last visit (**D**) are reported. The average measures for all combined individuals (SDS(SD)) were L: -2.3 (1.5); W: -2.0(1.0); OFC: -1.1(1.7); GW: 38.5(3.8) at birth and H: -1.7(1.3); W: -1.7(1.5); OFC: -2.4(1.8); BMI: -1(1.5) at last visit. **E**. Comparison of the growth parameters at last visit for patients carrying missense variants (black) compared to patients carrying other variants as well as deletions encompassing *NSD2* (red). \* = p-value <0.05 as tested by two-tailed Student's t-test. The

data in **C-E** are expressed as standard deviation score (SDS) based on the respective growth charts. Lines and whiskers represent mean $\pm$ SD. **F.** Linear correlation analysis between age and BMI and last visit.

Author Manuscript

Author Manuscript

Author Manuscript

Author Manuscript

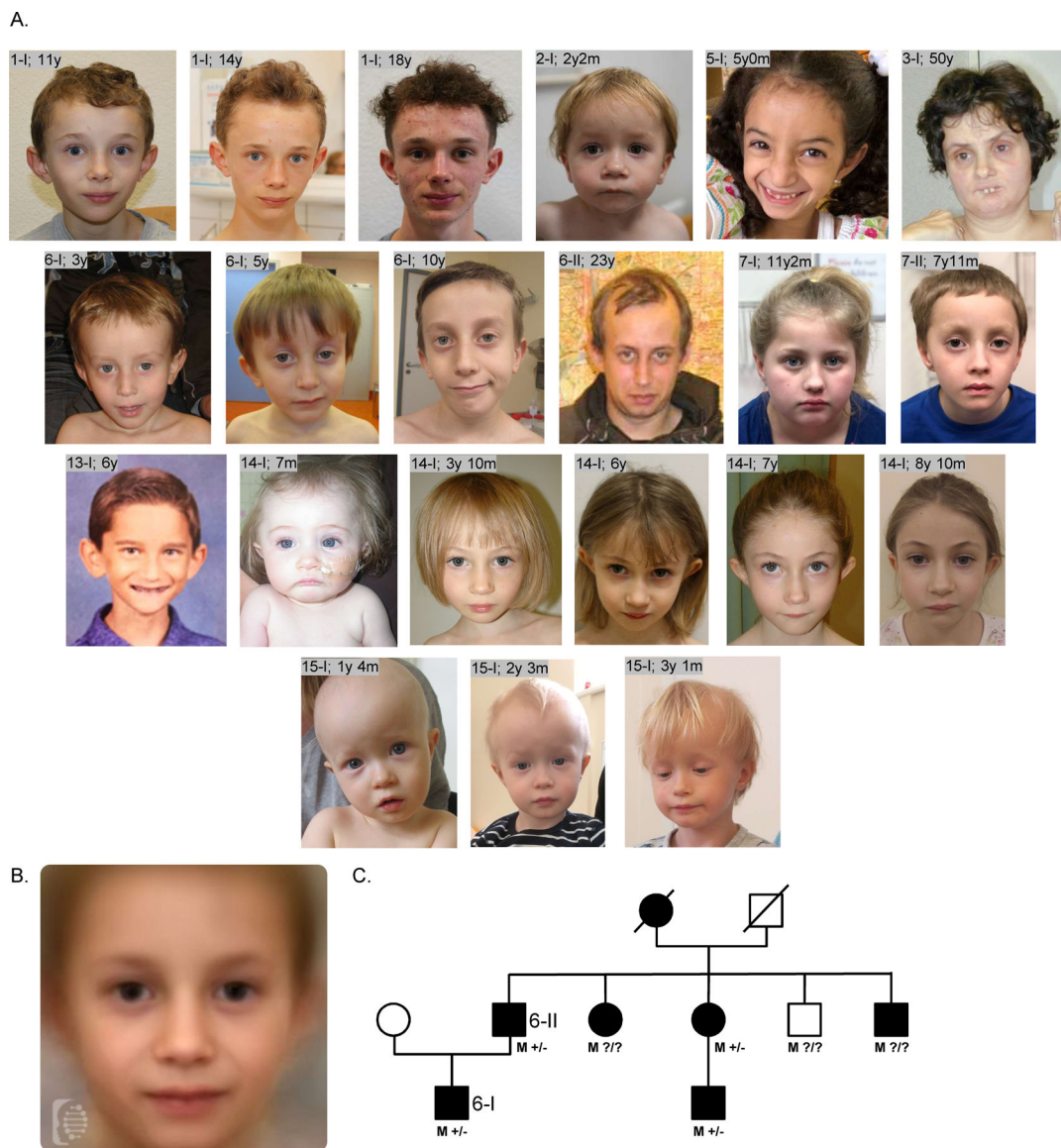


**Figure 4. Clinical data.**

**A.** Facial features of the affected individuals reported in this study. The age in years (y) and months (m) is reported beside each patient ID. **B.** Combined facial gestalt obtained by combining frontal photos using the Face2Gene online research tool (see methods and Web Resources sections). Photos from 12 different patients, including those depicted in **A**, were used for this purpose. **C.** Family tree of family number 6 in this study. M +/-/? = presence (+), absence (-) or unknown status (?) for the p.Asp1158Glyfs\*11 variant in each *NSD2* allele. Clinically affected individuals are shown as full symbols.